



SYNTHESIS, OPTOELECTRONIC PROPERTIES AND SINGLE-CRYSTAL X-RAY DIFFRACTOMETRY INVESTIGATION RESULTS OF SOME ARYLAMINE DERIVATIVES FOR OSC DEVICES

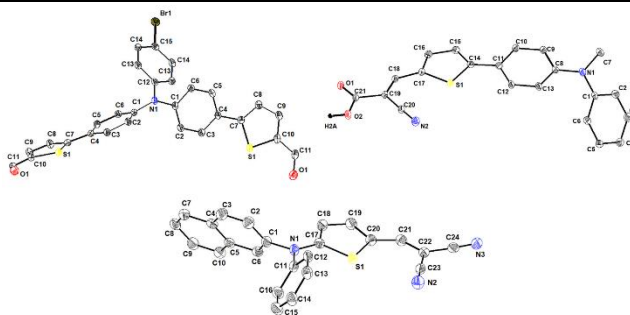
Natalia TEREŢI,^{a,b} Alexandra MORARU,^a Alexandra POP,^a Elena BOGDAN,^a Alexia Mihaela FRÎNCU,^a Niculina Daniela HĂDADE,^a Andreea Petronela CRIŞAN,^{a*} Anamaria TEREŢA^{a*} and Ion GROŞU^{a*}

^aBabeş-Bolyai University, Faculty of Chemistry and Chemical Engineering, Department of Chemistry and SOOMCC, Cluj-Napoca, 11 Arany Janos Street, 400028, Cluj-Napoca, Roumania

^bNational Institute for Research and Development of Isotopic and Molecular Technologies, 67-103 Donat Street, 400293 Cluj-Napoca, Roumania

Received May 23, 2025

The synthesis, absorption spectra in solution and thin films, the cyclic voltammetry, and single crystal X-ray diffractometry investigation results of some arylamine derivatives are discussed in the perspective of their utilisation as active materials in organic solar cells (OSCs).



INTRODUCTION

The continuous increase of energy consumption, the diminishing of the classic fossil combustible resources, and the requirements for reducing carbon emissions have greatly increased the interest in the development of green and cheap energy sources, and the valorisation of solar energy represents a valuable solution.¹ The classic inorganic solar cells (based on silicon chemistry) have already reached notoriety, being widely used to produce green electricity for domestic consumption or in large

amounts for commercial purposes (in solar parks).² Despite the significant advantages of silicon-based solar cells [e.g. high PCE (Power Conversion Efficiency) values, stability, industrial procedures], there are some limitations of these devices (e.g. high costs, negative environmental impact, high weight) which encourage the continuous investigations for alternative approaches.³

The innovative design of tailored band gap conjugated polymers,⁴ donors,⁵ and non-fullerene acceptors (NFAs)⁶ has strongly contributed to the spectacular development of donor/acceptor (D/A)

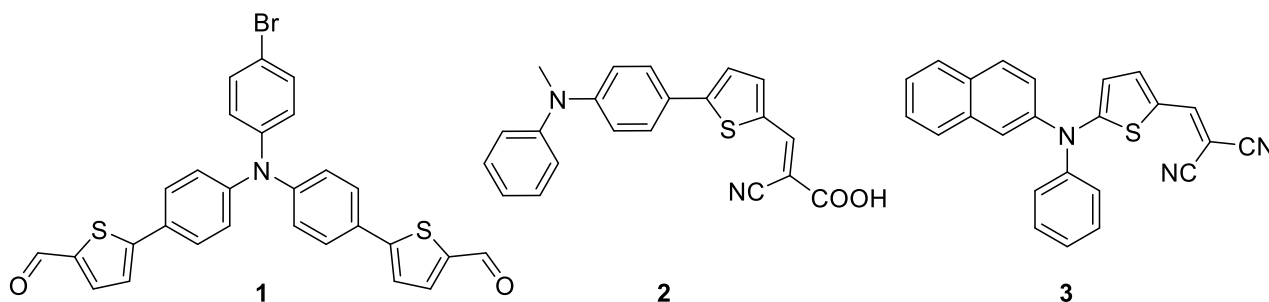
* Corresponding author: ion.grosu@ubbcluj.ro

bulk heterojunction (BHJ) OSCs, which reached Power Conversion Efficiency (PCE) values up to 20%. Despite the multiple advantages of OSCs (in the competition with classic silicon-based SCs), revealed by their low environmental impact, lightness, flexibility and transparency,¹ the industrial development of OSCs remained constrained by persistent problems of costs, scalability and stability of active materials.⁷

Small D-A (D- π -A) molecules which act alone as single active materials in the pioneering and surprising homojunction Single Material Organic Solar Cells (SMOSCs), despite the low reported PCE values (up to 1%), due to the high simplicity of the cells (direct or inverted), the high chemical stability and the low costs of the requested materials, became exciting targets for the research in the OSCs field.^{3,8} The main objectives for the investigations of homojunction SMOSCs are the elucidation of their working mechanism and the

understanding of structural requirements for the improvement of their PCE values.^{8,9}

A key feature of the performances of Homojunction Organic Solar Cells (HOSCs) is connected to the organisation of the active molecules in the solid state, which may favour the mobility of electrons or holes towards the electrodes and which strongly influences the efficiencies (PCE values) of OSCs.¹⁰ In this context and taking into account our experience in the investigation of supramolecular architectures built by hydrogen¹¹ or halogen¹² bonds, π - π stacking hydrophobic interactions¹³ and in the fabrication of OSC containing triarylamine-based active materials¹⁴ we considered of interest to investigate the solid-state structure obtained by single-crystal X-ray diffractometry of arylamine derivatives **1-3** (Scheme 1) which exhibit important structural units encountered in HOSC active materials.^{9,14c}



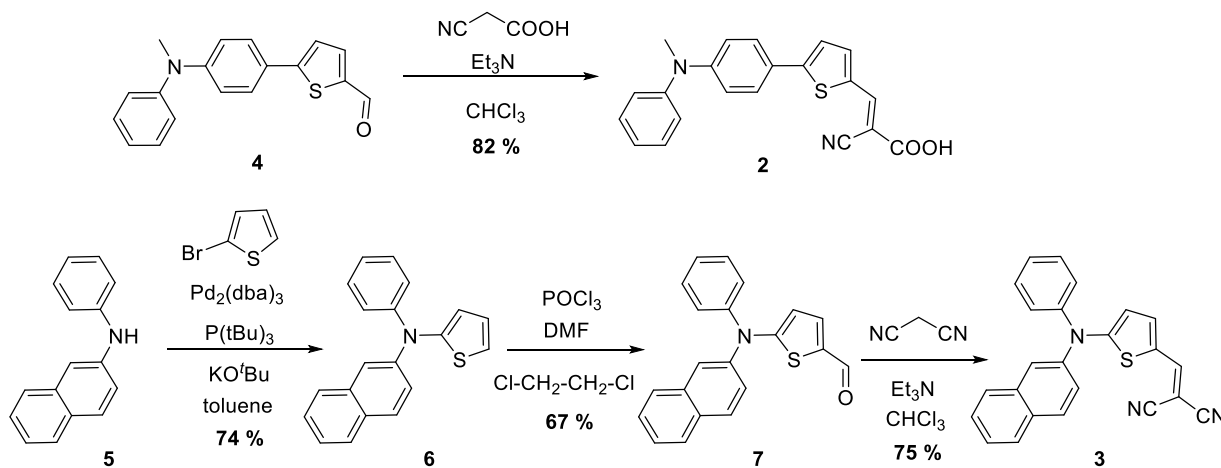
Scheme 1

RESULTS AND DISCUSSION

Access to compounds 1-3

Compounds **2** and **3** are new and were obtained

following the reactions presented in Scheme 2. The synthesis of compound **1** was already reported in the literature,¹⁵ but its optoelectronic properties and single-crystal X-ray diffractometry structure have not yet been explored.



Scheme 2

Aldehyde **4** and triarylamine **6** were already reported in the literature,^{16,17} but for the access to **6**, we have developed an original procedure based on the Buchwald coupling reaction of derivative **5** and 2-bromothiophene, employing Pd(0) as catalyst and KOtBu as base (Scheme 2). Aldehyde **7** was prepared *via* the Vilsmeier-Haack reaction of **6** with POCl₃ and DMF. Finally, the target compounds **2** and **3** were synthesised through the Knoevenagel condensation of aldehydes **4** and **7** with cyanoacetic acid and malononitrile, respectively, in chloroform using triethylamine as base (Scheme 2)

Optical and electrochemical properties of 1-3

The absorption properties of compounds **1-3** were studied both in dichloromethane solution and in thin films spun cast on glass from chloroform

solutions. Analysis of the absorption spectra of **1-3** (Fig. 1) revealed that all spectra exhibit a transition band in the 270–400 nm range (assigned to π - π^* interactions) and a more intense absorption band (with a maximum at 420 nm for compound **1** and around 480 nm for compounds **2** and **3**) corresponding to the internal charge transfer (ICT) band from the triarylamine donor unit to the various acceptor moieties. The ICT band of compound **1** appears blue-shifted relative to the spectra of **2** and **3** due to the weaker electron-withdrawing nature of the aldehyde group compared to dicyanovinyl or cyano, carboxyvinyl acceptor units. The absorption spectra of spin-coated films exhibit a bathochromic shift and broadening of the maximum absorption band, with the most pronounced effect for **2** (Fig. 1).

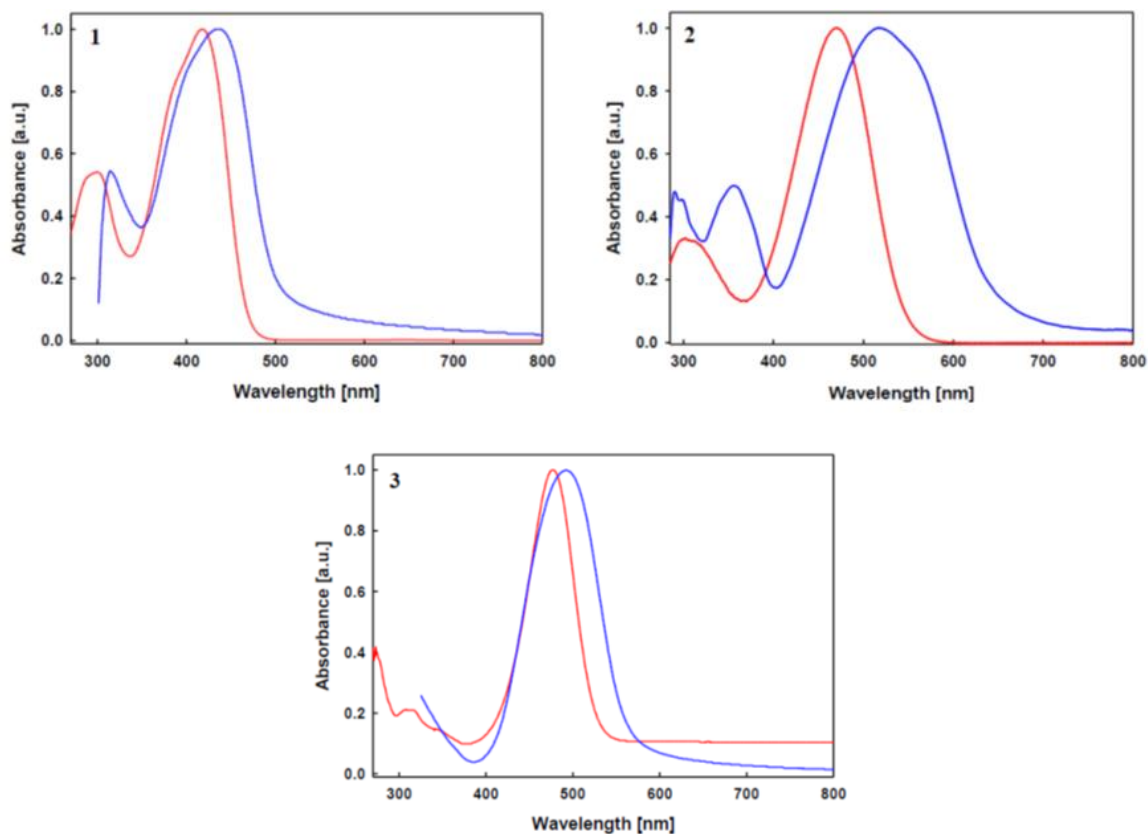


Fig. 1 – Normalized UV-Vis absorption spectra of target compounds **1-3**, in solution – red line and thin films – blue line.

The electrochemical behavior of **1-3** was studied using cyclic voltammetry in dichloromethane solution with Bu₄NPF₆ as supporting electrolyte. The cyclic voltammograms (CVs) of all three derivatives exhibit similar patterns, showing a reversible one-electron oxidation process with anodic peak potentials ranging from 0.9 to 1.2 V *vs.* SCE (Fig. 2, Table 1), corresponding to the formation of a stable radical cation. In the negative

potential region, an irreversible reduction process is observed, with cathodic peak potentials between –1.10 and –1.37 V *vs.* SCE, attributed to the reduction of the electron-withdrawing groups. The substitution of the methyl group with a β -naphthyl moiety and the direct attachment of the thiophene unit to the nitrogen atom of the donor block resulted in a 300 mV positive shift of E_{pa} , likely due to the greater steric hindrance of the naphthyl group

compared to the methyl group. Additionally, a ~ 250 mV negative shift of E_{pc} was observed,

which aligns with the stronger donor effect of the β -naphthyl group relative to the methyl one.¹⁸

Table 1
Optical and electrochemical data for compounds **1-3**: CH₂Cl₂ solutions (s); thin films on glass (f)

Cmpd	λ_{\max} (s) [nm]	λ_{\max} (f) [nm]	E_{pa} [V]	E_{pc} [V]
1	418	437	1.07	-1.10
2	470	520	0.92	-1.12
3	477	492	1.22	-1.37

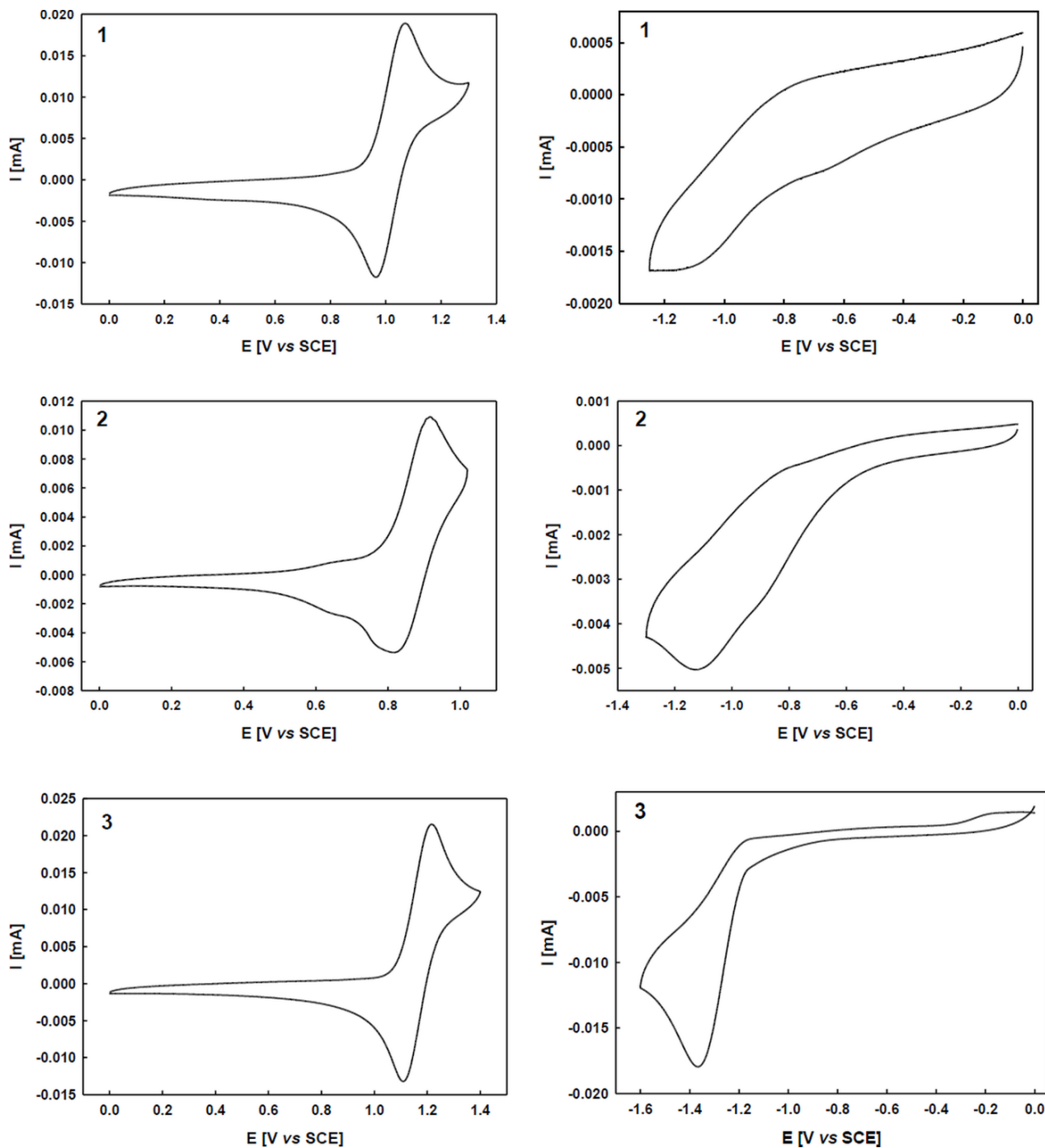


Fig. 2 – Cyclic voltammograms of target compounds **1-3** (1 mM in 0.10 M Bu₄NPF₆/CH₂Cl₂, scan rate 100 mV s⁻¹, Pt working electrode).

Single-crystal X-ray diffractometry structural investigation of 1-3

To gain further information about the solid-state molecular structure of compounds **1-3**, suitable crystals obtained by the slow evaporation of their chloroform solutions were investigated by single-crystal X-ray diffractometry.

The molecular structures of **1-3** are presented in Fig. 3. All compounds present an almost planar tri(di)arylamine central moiety with 120° bond angles around the nitrogen atom. In the case of the

triarylamine-containing derivatives **1** and **3**, a propeller-like geometry is observed around the central nitrogen atom, with the N-attached aryl groups rotated at angles ranging from 56° to 65° . In the case of compound **2**, the unsubstituted phenyl group at nitrogen is also rotated by 56° , while the *p*-substituted phenyl unit is only slightly deviated (7°) from the C(Me)–N–C(Ph) plane. Another common feature is that, aside from the aryl rings of the tri(di)arylamine unit, the molecules display a quasi-planar conformation of the thiophene-containing moieties.

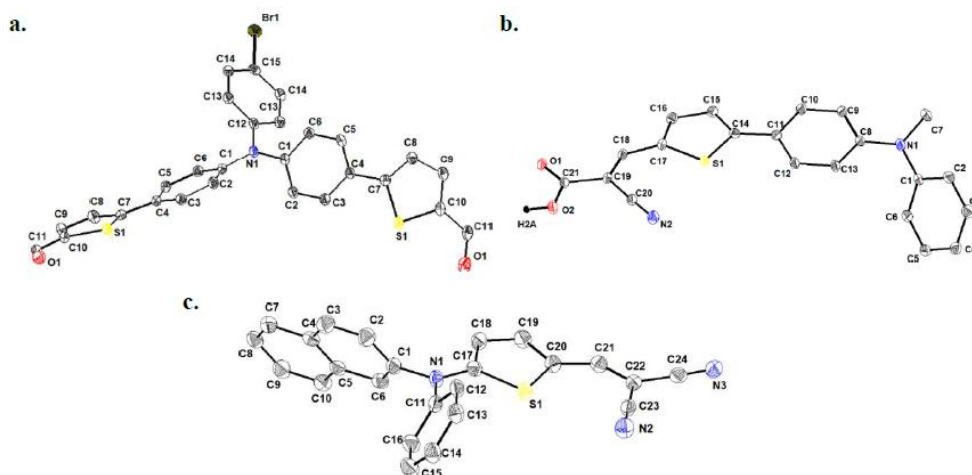


Fig. 3 – ORTEP representation (50% probability level of atomic displacement ellipsoids) of the molecular structure of compounds **1** (a), **2** (b), and **3** (c). Hydrogen atoms were omitted for clarity.

In compound **1**, the dihedral angle between the inner phenyl ring and the thiophene one is only 2.04° , while the carbonyl bond is coplanar with the thiophene unit. Investigation of the molecular packing pattern revealed the formation of parallel 2D sheets via strong C–H \cdots π intermolecular interactions (H14 \cdots Cg2 [Cg2 = C1–C6 phenyl] distance of 2.75 \AA , depicted in pink in Fig. 4) that

are further connected in a head-to-tail manner in a 3D architecture.

The carbonyl oxygen atom is responsible for many of the intermolecular interactions detected in the lattice: multiple O1 \cdots Cg2 short contacts (3.223 \AA in pink) and H-bonds with H8 of the thiophene rings (H8 \cdots O1 distance is 2.59 \AA , depicted in orange in Fig. 4), leading to a compact packing.

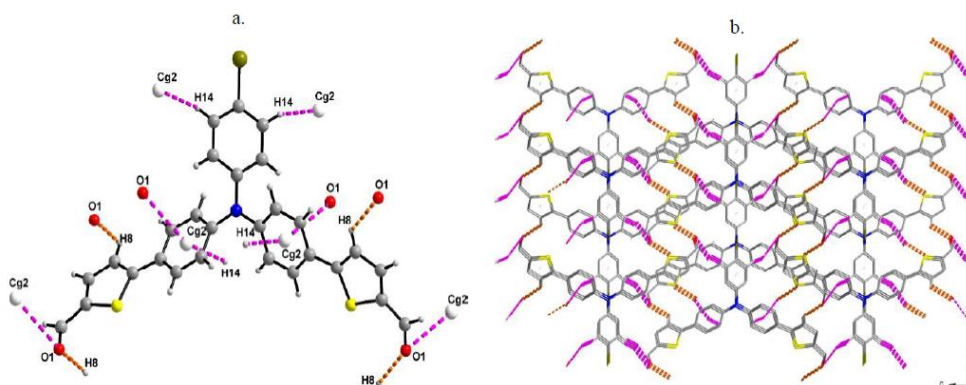


Fig. 4 – a) Detailed intermolecular interactions; b) packing patterns of compound **1** in the lattice. Hydrogen atoms were omitted for clarity, except when involved in interactions.

In compound **2**, there is a slightly higher deviation from the coplanarity for the thiophene-containing part: a 7.7° torsion angle between the methyl group and the inner phenyl ring, and a 10.35° rotation between the latter and the thiophene ring. The acceptor part is coplanar with the thiophene unit, and supplemental reinforcing interactions are observed with neighbouring atoms: S1 \cdots H12 distance is 2.669 Å and S1 \cdots N2 distance is 3.327 Å (depicted in green in Fig. 5a). Association

into head-to-tail dimers by strong doubled H-bonds O2–H2A \cdots O1 (1.747 Å, depicted in red in Fig. 5) is observed. These dimers are further connected to other dimers by C–H \cdots π interactions (H4 \cdots Cg1 [Cg1 = thiophene] distance of 2.760 Å and H12 \cdots Cg2 [Cg2 = C1–C6 phenyl] distance of 2.938 Å, depicted in pink in Fig. 5) and H \cdots N contacts with the nitril group (H9 \cdots N2 distance of 2.552 Å, depicted in orange in Fig. 5) in a V-shaped manner at a 51.69° angle.

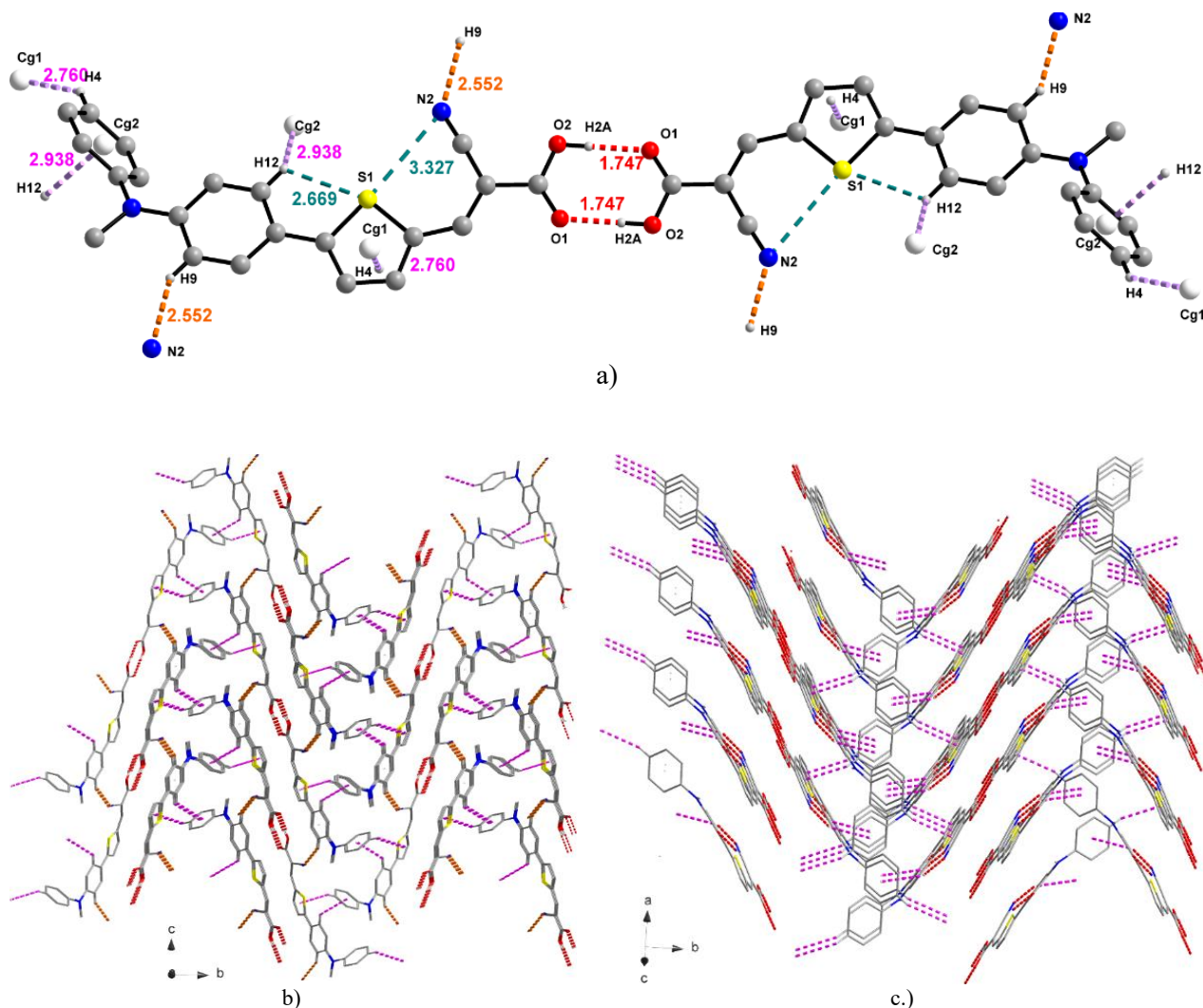


Fig. 5 – a) Detailed intermolecular contacts; b) packing patterns (a-axis view); c) formation of V-shaped associations via intermolecular interactions of compound **2** in the lattice. Hydrogen atoms were omitted for clarity, except when involved in interactions.

The structure of derivative **3** shows again a high degree of planarity for the dicyanovinyl moiety and the thiophene ring. The molecules arrange themselves in a head-to-tail manner into dimers via H-bonding of the nitrile groups (H12 \cdots N3 distance of 2.594 Å, depicted in orange in Fig. 6). Furthermore, a plethora of C–H \cdots π interactions

connecting the above-mentioned dimers reinforce the 3D crystalline structure (H14 \cdots Cg2 [Cg2 = C1–C6 naphthyl] distance of 2.831 Å, H15 \cdots Cg3 [Cg3 = C5–C4–C7–C8–C9–C10 naphthyl] distance of 2.890 Å, and H2 \cdots Cg4 [Cg4 = C11–C16 phenyl] distance of 2.853 Å, depicted in pink in Figure 6) in a highly organised lattice.

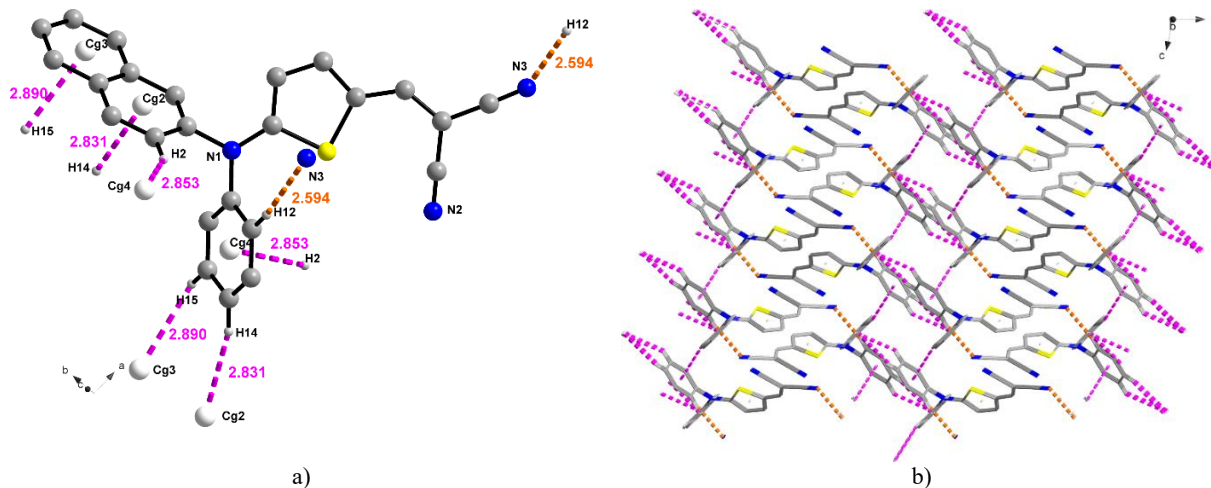


Fig. 6 – a) Detailed intermolecular contacts; b) packing (b-axis view) of compound **3** in the lattice. Hydrogen atoms were omitted for clarity, except when involved in interactions.

EXPERIMENTAL

General considerations

All reagents and chemicals from commercial sources were used without further purification. Reactions were carried out under an argon atmosphere unless otherwise stated. Solvents were dried and purified using standard techniques. Thin layer chromatography was performed on Silica gel 60 chromatography plates F254. Column chromatography separations were performed using analytical-grade solvents and appropriate silica gel (pore size 60 Å). The visualisation of chromatographic plates was performed by UV detection (254 nm) or by staining with 2,4-dinitrophenylhydrazine or KMnO_4 solutions. NMR spectra were recorded with a Bruker AVANCE III 600 (^1H , 600 MHz and ^{13}C , 150 MHz). Chemical shifts are given in ppm relative to TMS, and coupling constants J are given in Hz. High resolution mass spectra (HRMS) in positive ion mode were recorded using APCI or electrospray ionisation modes with a LTQ XL Orbitrap ThermoScientific mass spectrometer. UV–Vis measurements were performed in various solvents (HPLC grade) at room temperature using a Shimadzu UV spectrophotometer (UV-1800). Cyclic voltammetry investigations were carried out in dichloromethane (HPLC grade). Tetrabutylammonium hexafluorophosphate was purchased from Aldrich and was used without purification. Solutions were deaerated by argon bubbling prior to each experiment. Experiments were conducted in a one-compartment cell equipped with platinum and saturated calomel (reference)

electrodes (SCE) with a Biologic SP-150 potentiostat with positive feedback compensation.

Procedures for the synthesis of compounds **2** and **3**

Procedure for the synthesis of 2. To a stirred solution of cyanoacetic acid (eq. 1.3) and carbaldehyde **4** (eq. 1) in CHCl_3 , a small amount (3–5 drops) of Et_3N was added dropwise. The mixture was then refluxed under an argon atmosphere for 20 hours. Afterwards, the solvent was evaporated under reduced pressure, and the resulting residue was purified by column chromatography on silica gel using a 10:0.4 DCM/THF elution system. The desired compound **2** was separated ($R_f = 0.6$ in tetrahydrofuran) as a fine dark red powder in 82% yield.

Procedure for the synthesis of 3. In a round-bottom flask equipped with a magnetic stirrer and a reflux condenser, 350 mg of compound **7** (1.06 mmol) and 77.2 mg of malononitrile (1.17 mmol) were dissolved in 30 mL chloroform. Triethylamine was added dropwise until the solution turned reddish. The mixture was heated to 100°C in an oil bath, and the reaction was monitored by TLC. Once the starting material was fully consumed, heating was stopped, the solvent was evaporated, and the crude product was purified by chromatography, yielding 300 mg of compound **3** as a red solid [75% yield, $R_f = 0.7$ (dichloromethane, silica gel)].

Procedure for the synthesis of 6. In a two-neck flask, *N*-phenylnaphthalen-2-amine **5** (1.5 g, 6.84 mmol), 2-bromothiophene (0.66 mL, 6.84 mmol), and sodium *tert*-butoxide (1.97 g,

20.5 mmol) were dissolved in 100 mL of anhydrous toluene and degassed for 20 min. Tris(dibenzylideneacetone)dipalladium (0.24 g, 4 mol%) and tri-*tert*-butylphosphine (0.4 mL, 1.7 mmol) were then added, and the reaction was refluxed under argon for 15 h.

After cooling, the solvent was removed under reduced pressure, and the crude product was dissolved in dichloromethane, washed with water (2x30mL) and brine (30 mL), dried over MgSO₄, and evaporated. Purification by silica gel column chromatography (petroleum ether/dichloromethane, 4:1) yielded 1.52 g of the target compound (74% yield).

Procedure for the synthesis of 7. To a solution of compound **6** (400 mg, 1.3 mmol) in 50 mL 1,2-dichloroethane, phosphoryl chloride (0.18 mL, 1.9 mmol) and *N,N'*-dimethylformamide (0.2 mL, 2.6 mmol) were slowly added. The mixture was refluxed for 4 h, and the reaction was monitored by thin-layer chromatography. Once complete, the reaction mixture was cooled to room temperature, diluted with 50 mL of dichloromethane, and quenched with 50 mL of saturated sodium acetate solution. After stirring for 20 min, the mixture was extracted twice with dichloromethane (50 mL). The organic phase was washed with water (2x30 mL) and brine (30 mL), dried over MgSO₄, and filtered. The solvents were removed under reduced pressure, and the purification of the product was carried out by column chromatography, yielding 350 mg of compound **7** as a yellow solid [67% yield, R_f = 0.3 (dichloromethane, silica gel)].

Characterisation of compounds

(2-cyano-3-(5-(4-(methyl(phenyl)amino)phenyl)thiophen-2-yl)acrylic acid 2. Dark red solid (0.4 g, 82 %), mp = 198–200 °C (R.f = 0.6 in tetrahydrofuran). ¹H NMR (600MHz, DMSO-d₆) δ (ppm): 3.33 (s, 3H), 6.91 (d, 2H, *J* = 8.8 Hz), 7.17 (t, 1H, *J* = 7.5 Hz), 7.23 (d, 2H, *J* = 7.6 Hz), 7.41 (dd, 2H, *J* = 8.2 Hz, *J* = 7.6 Hz), 7.60 (d, 1H, *J* = 4.1 Hz), 7.64 (d, 2H, *J* = 8.7 Hz), 7.97 (d, 1H, *J* = 4.1 Hz), 8.45 (s, 1H). ¹³C NMR (150MHz, DMSO-d₆) δ (ppm): 96.5, 116.3, 116.8, 122.5, 123.2, 124.3, 127.4, 129.7, 132.8, 142.1, 146.7, 147.4, 149.8, 154.3, 163.9.

2-((5-(naphthalen-2-yl(phenyl)amino)thiophen-2-yl)methylene)malononitrile 3. Red solid (0.3 g, 75%), mp = 124–125 °C (R.f = 0.7 in dichloromethane). ¹H NMR (600MHz, CDCl₃) δ (ppm): 6.44 (d, 1H, *J* = 4.6 Hz), 7.32 (t, 1H, *J* = 7.2 Hz),

7.36 (d, 2H, *J* = 7.8 Hz), 7.38 (dd, 1H, *J* = 8.8 Hz, *J* = 2.2 Hz), 7.42–7.45 (overlapped peaks, 3H), 7.49 (s, 1H), 7.50–7.53 (overlapped signals, 2H), 7.75–7.76 (overlapped signals, 2H), 7.85 (m, 1H), 7.88 (d, 1H, *J* = 8.8 Hz). ¹³C NMR (150 MHz, CDCl₃) δ (ppm): 112.8, 115.0, 116.0, 122.8, 123.8, 123.9, 125.9, 126.7, 127.2, 127.5, 127.8, 127.9, 130.2, 130.3, 132.0, 133.9, 142.5, 145.2, 149.4, 166.7.

***N*-(naphthalen-2-yl)-*N*-phenylthiophen-2-amine 6.** White solid (1.52 g, 74 %), mp = 97–98 °C (R.f = 0.5 in petroleum ether / dichloromethane = 4 / 1). ¹H NMR (600MHz, CDCl₃) δ (ppm): 6.77 (d, 1H, *J* = 3.6 Hz), 6.92 (t, 1H, *J* = 4.6 Hz), 7.03 (d, 1H, *J* = 5.6 Hz), 7.06 (td, 1H, *J* = 7.4 Hz, *J* = 1.2 Hz), 7.18 (m, 2H), 7.29 (m, 2H), 7.34 (m, 1H), 7.37 (dd, 1H, *J* = 8.2 Hz, *J* = 1.2 Hz), 7.41 (m, 1H), 7.47 (t, 1H, *J* = 1.8 Hz), 7.63 (d, 1H, *J* = 8.2 Hz), 7.73 (d, 1H, *J* = 8.8 Hz), 7.76 (d, 1H, *J* = 8.2 Hz). ¹³C-RMN (150 MHz, CDCl₃) δ (ppm): 118.7, 121.0, 121.7, 122.7, 122.9, 123.1, 124.7, 126.1, 126.5, 127.2, 127.7, 129.0, 129.3, 130.1, 134.3, 145.7, 148.1, 151.6.

5-(naphthalen-2-yl(phenyl)amino)thiophene-2-carbaldehyde 7. Yellow solid (0.35 g, 67 %), mp = 55–56 °C (R.f = 0.3 in dichloromethane). ¹H NMR (600MHz, CDCl₃) δ (ppm): 6.45 (d, 1H, *J* = 4.8 Hz), 7.23 (m, 1H), 7.33 (m, 2H), 7.36–7.40 (overlapped signals), 7.46–7.48 (overlapped signals, 2H), 7.71–7.74 (overlapped signals, 2H), 7.82–7.84 (overlapped signals, 2H), 9.63 (s, 1H). ¹³C NMR (150 MHz, CDCl₃) δ (ppm): 112.9, 123.2, 124.2, 125.7, 126.3, 126.4, 127.0, 127.7, 127.9, 130.0, 130.1, 130.9, 131.7, 134.1, 138.4, 143.6, 146.2, 164.2, 181.5.

Crystal structure determination. Details about the crystal structure determination and refinement data are provided in Table 2. The crystals of **1** – **3** were mounted on MiTeGen microMounts cryoloops, and data were collected on a Bruker D8 VENTURE diffractometer using Mo-Kα radiation (λ = 0.71073 Å) from a IμS 3.0 microfocus source with multilayer optics, at low temperature. Hydrogen atoms were placed in fixed, idealised positions and were refined with a riding model and a mutual isotropic thermal parameter. The structures were refined with anisotropic thermal parameters for non-H atoms. For structure solving and refinement, the Bruker APEX4 and APEX5 Software Packages were used.¹⁹ Drawings were created using the Diamond program.²⁰ The CCDC reference numbers are 2453014 (**1**), 2453015 (**2**) and 2453016 (**3**). The supplementary

crystallographic data for this article can be obtained free of charge from The Cambridge

Crystallographic Data Centre via <https://www.ccdc.cam.ac.uk/structures/>.

Table 2

Crystal data and structure refinement for **1**, **2** and **3**

Compound	1	2	3
Molecular formula	C ₂₈ H ₁₈ BrNO ₂ S ₂	C ₂₁ H ₁₆ N ₂ O ₂ S	C ₂₄ H ₁₅ N ₃ S
Formula weight	544.46	360.42	377.45
Crystal size / mm ³	0.016 × 0.094 × 0.119	0.008 × 0.100 × 0.120	0.019 × 0.075 × 0.128
Crystal habit	yellow	orange	yellow
$\lambda(\text{MoK}\alpha) / \text{\AA}$	0.71073	0.71073	0.71073
T / K	100.(2)	100.(2)	100.(2)
Crystal system	monoclinic	monoclinic	monoclinic
Space group	<i>C2/c</i>	<i>P21/c</i>	<i>P21/c</i>
$a / \text{\AA}$	8.2351(3)	6.0792(3)	15.2180(9)
$b / \text{\AA}$	11.4104(4)	26.5015(15)	11.5976(6)
$c / \text{\AA}$	23.8202(11)	10.7994(6)	10.7859(6)
$\alpha / ^\circ$	90	90	90
$\beta / ^\circ$	94.386(2)	104.831(2)	102.397(2)
$\gamma / ^\circ$	90	90	90
$V / \text{\AA}^3$	2231.73(15)	1681.91(16)	1859.24(18)
Z	4	4	4
$D_{\text{calc}} / \text{g cm}^{-3}$	1.620	1.423	1.348
μ / mm^{-1}	2.058	0.211	0.188
θ range for data collections ($^\circ$)	3.06–28.30	2.48–28.38	2.23–26.37
$F(000)$	1104	752	784
$T_{\text{max}} / T_{\text{min}}$	0.83 / 0.97	0.95 / 0.98	0.92 / 1.0
Refl. collected / unique / R_{int}	28726 / 0.0481	44029 / 0.0348	50056 / 0.1155
Completeness to θ	99.9%	99.7%	100%
Refinement method	Full-matrix least-squares on F^2		
Data / restraints / parameters	2781 / 0 / 156	4197 / 0 / 241	3807 / 0 / 253
Goodness-of-fit, S	1.087	1.038	1.056
Final R indices [$I > 2\sigma(I)$]	$R_1 = 0.0304$	$R_1 = 0.0329$	$R_1 = 0.0522$
	$wR_2 = 0.0714$	$wR_2 = 0.0801$	$wR_2 = 0.0948$
R indices (all data)	$R_1 = 0.0420$	$R_1 = 0.0368$	$R_1 = 0.0896$
	$wR_2 = 0.0774$	$wR_2 = 0.0836$	$wR_2 = 0.1110$
$\Delta\rho_{\text{max}}, \Delta\rho_{\text{min}} / e \text{\AA}^{-3}$	0.424 / –0.584	0.368 / –0.358	0.423 / –0.264
CCDC No.	2453014	2453015	2453016

CONCLUSIONS

The investigation of UV-Vis spectra of three D- π -A arylamine derivatives revealed bathochromic shifts for the compounds with better acceptor units [dicyanovinyl (**3**) and carboxy, cyanovinyl (**2**) *versus* formyl (**1**)] and for the spectra recorded for the thin films on glass *versus* the spectra of the same compound recorded in solution. The single crystal X-ray diffractometry investigations pointed out a propeller-like disposition of the aryl units and an almost planar structure for the phenylene-thiophene units. In the lattices, the molecules are connected *via* many hydrogen bonds and π - π stacking contacts, leading

to spectacular arrangements. However, no formation of zones with segregations of donor and acceptor moieties, favorable for the HOSC behavior, were observed.

Acknowledgements. Financial support by the Roumanian National Authority for Scientific Research and Innovation, CNCS-UEFISCDI, projects number PN-III-P4-ID-PCE-2020-1812 and COFUND-M-ERANET-3-COFFEE-317, is gratefully acknowledged.

REFERENCES

1. A. Labrunie, A. H. Habibi, S. Dabos-Seignon, P. Blanchard, C. Cabanetos, *Dyes Pigm.* **2019**, *170*, 10763.

2. P. K. Nayak, S. Mahesh, H. J. Snaith, D. Cahen, *Nat. Rev. Mater.* **2019**, *4*, 269.
3. J. Roncali, I. Grosu, *Adv. Sci.* **2019**, *6*, 1801026.
4. a) J. Roncali, *Macromol. Rapid Commun.* **2007**, *28*, 1761; b) J. Chen, Y. Cao, *Acc. Chem. Res.* **2009**, *42*, 1709; c) Y.-J. Cheng, S.-H. Yang, C.-S. Hsu, *Chem. Rev.* **2009**, *109*, 5868.
5. a) A. Mishra, P. Bäuerle, *Angew. Chem., Int. Ed.* **2012**, *51*, 2020; b) J. Roncali, P. Leriche, P. Blanchard, *Adv. Mater.* **2014**, *26*, 3821; c) S. D. Collins, N. A. Ran, M. C. Heiber, T.-Q. Nguyen, *Adv. Energy Mater.* **2017**, 1602242; d) A. Venkateswararao, K.-T. Wong, *Bull. Chem. Soc. Jpn.* **2021**, *94*, 812
6. a) A. F. Eftaiha, J.-P. Sun, I. G. Hill, G. C. Welch, *J. Mater. Chem. A* **2014**, *2*, 1201; b) Y. Lin, J. Wang, Z.-G. Zhang, H. Bai, Y. Li, D. Zhu, X. Zhan, *Adv. Mater.* **2015**, *27*, 1170; c) G. Zhang, J. Zhao, P. C. Y. Chow, K. Jiang, J. Zhang, Z. Zhu, J. Zhang, F. Huang, H. Yan, *Chem. Rev.* **2018**, *118*, 3447
7. a) R. Po, G. Bianchi, C. Carbonera, A. Pellegrino, *Macromol.* **2015**, *48*, 453; b) R. Po, J. Roncali, *J. Mater. Chem. C* **2016**, *4*, 3677; c) J. Min, Y. Luponosov, C. Cui, B. Kan, H. Chen, X. Wan, Y. Chen, S. A. Ponomarenko, Y. Li, C. J. Brabec, *Adv. Energy Mater.* **2017**, *7*, 1700465
8. J. Roncali, *Adv. Energy Mater.* **2021**, *47*, 2102987
9. N. Terenti, G.I. Giurgi, C. Anghel, A. Bogdan, A. Pop, I. Stroia, A. Terec, L. Szolga, I. Grosu, J. Roncali, *J. Mater. Chem. C* **2022**, *10*, 5716
10. J. Fu, Q. Yang, P. Huang, S. Chung, K. Cho, Z. Kan, H. Liu, X. Lu, Y. Lang, H. Lai, F. He, P. W. K. Fong, S. Lu, Y. Yang, Z. Xiao, G. Li, *Nat. Commun.* **2024**, *15*, 1830
11. a) M. Cîrcu, V. Paşcanu, A. Soran, B. Braun, A. Terec, C. Socaci, I. Grosu, *CrystEngComm* **2012**, *14*, 632; b) N. Toşa, A. Bende, R. A. Varga, A. Terec, I. Bratu, I. Grosu, *J. Org. Chem.* **2009**, *74*, 3944
12. a) L. Pop, I. G. Grosu, M. Miclăuş, N. D. Hădăde, A. Pop, A. Bende, A. Terec, M. Bărboiu, I. Grosu, *Cryst. Growth Des.* **2021**, *21*, 1045; b) I. G. Grosu, L. Pop, M. Miclăuş, N. D. Hădăde, A. Terec, A. Bende, C. Socaci, M. Bărboiu, I. Grosu, *Cryst. Growth Des.* **2020**, *20*, 3429; c) M. Balog, I. Grosu, G. Plé, Y. Ramondenc, E. Condamine, R. Varga, *J. Org. Chem.* **2004**, *69*, 1337; d) F. Piron, N. Vanthuyne, B. Joulin, J.-V. Naubron, C. Cismaş, A. Terec, R. A. Varga, C. Roussel, J. Roncali, I. Grosu, *J. Org. Chem.* **2009**, *74*, 9062; e) M. I. Rednic, R. A. Varga, A. Bende, I. G. Grosu, M. Miclăuş, N. D. Hădăde, A. Terec, E. Bogdan, I. Grosu, *Chem. Commun.* **2016**, 52, 12322
13. a) N. Bogdan, E. Condamine, L. Toupet, Y. Ramondenc, E. Bogdan, I. Grosu, *J. Org. Chem.* **2008**, *73*, 5831; b) N. Bogdan, I. Grosu, G. Benoît, L. Toupet, Y. Ramondenc, E. Condamine, I. Silaghi-Dumitrescu, G. Plé, *Org. Lett.* **2006**, *8*, 2619; c) L. Pop, F. Dumitru, N. D. Hădăde, Y.-M. Legrand, A. Van der Lee, M. Bărboiu, I. Grosu, *Org. Lett.* **2015**, *17*, 3494; d) Diac, A., Matache, M., Grosu, I., Hădăde, N.D. *Adv. Synth. Catal.* **2018**, *360*, 817
14. a) D. Demeter, S. Mohamed, A. Diac, I. Grosu, J. Roncali, *ChemSusChem* **2014**, *7*, 1046; b) D.-F. Bogoşel, G.-I. Giurgi, A. Balan, A. Pop, I. Grosu, A.P. Crişan, A. Terec, *Org. Electron.* **2025**, *141*, 107212; c) A. P. Diac, L. Szolga, C. Cabanetos, A. Bogdan, A. Terec, I. Grosu, J. Roncali, *Dyes Pigm.* **2019**, *171*, 107748
15. J. Shi, Z. Chai, R. Tang, J. Hua, Q. Li, Z. Li, *Sci. China Chem.* **2015**, *58*, 1144
16. Y. Jiang, C. Cabanetos, M. Allain, P. Liu, J. Roncali, *J. Mater. Chem. C* **2015**, *3*, 5145
17. H. Hartmann, P. Gerstner, D. Rohde, *Org. Lett.* **2001**, *3*, 1673
18. S. Mohamed, D. Demeter, J.-A. Laffitte, P. Blanchard, J. Roncali, *Sci. Rep.* **2015**, *5*, 9031
19. G. M. Sheldrick, *Acta Crystallogr., Sect. C: Struct. Chem.* **2015**, *C71*, 3
20. DIAMOND – Visual Crystal Structure Information System, CRYSTAL IMPACT, Postfach 1251, 53002 Bonn, Germany, 2001.